The Science of Nature (2024) 111:10
https://doi.org/10.1007/s00114-024-01893-w

ORIGINAL ARTICLE

Life in a Central European warm-temperate to subtropical open forest: Paleoecology of the rhinocerotids from Ulm-Westtangente (Aquitanian, Early Miocene, Germany)

Manon Hullot[1] · Céline Martin[2] · Cécile Blondel[3] · Gertrud E. Rössner[1,4]

Received: 2 November 2023 / Revised: 15 January 2024 / Accepted: 17 January 2024 / Published online: 14 February 2024
© The Author(s) 2024

Abstract

The Ulm-Westtangente locality has yielded the most abundant vertebrate fauna from the Aquitanian stage in Germany. Its dating to the Mammal Neogene Zone 2a, a turnover in Cenozoic climate, makes it a crucial source for the understanding of faunal, paleoecological and paleoenvironmental specifics of the European Aquitanian. However, while most taxa from Ulm-Westtangente have been studied, little to no research has been conducted on the large herbivores, particularly on the two rhinocerotids *Mesaceratherium paulhiacense* and *Protaceratherium minutum*. Here, we used a multi-proxy approach to investigate the paleoecology of these two species. The remains of the smaller species *P. minutum* (438 to 685 kg) are twice as abundant as those of the larger *M. paulhiacense* (1389 to 2327 kg), but both display a similar age structure (~ 10% of juveniles, 20% of subadults and 70% of adults), mortality curves, and mild prevalence of hypoplasia (~ 17%). Results from dental mesowear, microwear, and carbon isotopes indicate different feeding preferences: both were C3 feeders but *M. paulhiacense* had a more abrasive diet and was probably a mixed feeder. Our study on rhinocerotids also yielded new paleoenvironmental insights, such as the mean annual temperature (15.8 °C) and precipitation (317 mm/year) suggesting rather warm and dry conditions.

Keywords Diet · Habitat · Niche partioning · Freshwater Molasse Germany

Introduction

The Early Miocene was a key period in Rhinocerotidae evolution marked by significant diversification and geographic expansion. Indeed, the family experienced a peak of alpha-diversity during late Early Miocene with several sympatric species at single fossil sites (Antoine and Becker 2013). The early Miocene was also characterized by a turnover and a high degree of endemism in rhinoceros species of Western Europe. Yet, the paleoecology of rhinocerotids during this important time period has rarely been studied, although it has the potential to reveal niche partioning and ecological shifts associated with climatic conditions (Hullot et al. 2023a, b).

Ulm-Westtangente in Germany is one of the richest fossil mammal localities of the Early Miocene (Aquitanian: 23.04 – 20.44 Mya; Raffi et al. 2020) in Europe (Heizmann et al. 1989; Costeur et al. 2012). This fossil site is located in the Lower Freshwater Molasse sediments of the Baden-Württemberg Basin in Southwestern Germany, about 5 km North-West of Ulm (590 m above sea level, coordinates:

Communicated by: Aurora Grandal d'Anglade

✉ Manon Hullot
manon.hullot@gmail.com

[1] SNSB - Bayerische Staatssammlung für Paläontologie und Geologie, Richard-Wagner-Straße 10, 80333 Munich, Germany

[2] Géosciences Montpellier, Université de Montpellier, Campus Triolet cc060, Bât 22 – Place Eugène Bataillon, 34095 Montpellier cedex 5, France

[3] PALEVOPRIM Poitiers, Université de Poitiers Bât B35 – TSA 51106, 6 Rue Michel Brunet, 86073 Poitiers, France

[4] Department für Geo- und Umweltwissenschaften, Paläontologie & Geobiologie, Ludwig-Maximilians-Universität München, Richard-Wagner-Straße 10, 80333 Munich, Germany

48.418321 N, 9.933701 E – converted from the Gauss Kruger coordinates in original publication of Heizmann et al. 1989: r 35 69 188, h 53 64 925). It has been dated to the Early Miocene by correlation with the Mammal Neogene-Zone 2a (MN2a; Bruijn et al. 1992; Steininger 1999). The MN2 displayed relatively warm and stable climatic conditions, following the cold start of the Miocene (MN1) caused by the Mi-1 glaciation event (Zachos et al. 2001; Westerhold et al. 2020). A single 35 cm-thick layer has yielded more than 60 mammal species, making it the most abundant vertebrate fauna from the Early Miocene ever found in Germany (Heizmann et al. 1989; Costeur et al. 2012). Among the numerous fossil remains excavated (~ 6000 from large mammals, > 6000 from small mammals, and > 1000 from other vertebrates; Heizmann et al. 1989), abundant material was attributed to two species of rhinocerotids: the small tapir-sized *Protaceratherium minutum*, and the medium to large sized *Mesaceratherium paulhiacense*. Several taxa have been well studied at the locality, including: rodents and lagomorphs (Werner 1994), eulipotyphlas (Ziegler 1989, 1990a, b), suids (Hellmund 1991), carnivores: (Heizmann and Morlo 1994; Peigné and Heizmann 2003), or lizards (Klembara et al. 2017). However, this is not the case of large herbivores, and notably the rhinocerotids.

The locality of Ulm-Westtangente thus provides a unique opportunity to investigate rhinocerotid paleoecology at a key moment of their evolutionary history. Here, we use a multi-proxy approach including diet proxies at different time scales ($\delta^{13}C$, first years of life; dental microwear, last days to months; and mesowear, general lifetime), habitat proxies ($\delta^{18}O$ and $\delta^{13}C$: temperature, precipitation, habitat openness), and life history proxies (enamel hypoplasia, body mass prediction, mortality curves: metabolic and environmental stresses, age structure, vulnerability periods). The combination of independent methods aims to produce more robust results by compensating for the weaknesses of individual approaches. This has the potential to reveal new aspects and refine complex patterns. Based on this, niche partitioning can be discussed, to propose paleoenvironmental interpretations, and to provide new data for the understanding of the faunal turnover around the Oligocene–Miocene transition and the early diversification of the Rhinocerotidae in Europe.

Abbreviations

Capital letters are used for the upper teeth (D: deciduous molar; P: premolar; M: molar), while lower case letters indicate lower teeth (d, p, m). Institutional abbreviations: SMNS – Staatliches Museum für Naturkunde Stuttgart, Germany

Materials and methods

The material studied is curated at the SMNS. It is composed of a total of 492 teeth: 337 of *Protaceratherium minutum* (137 isolated teeth; 200 from four skulls, two maxillae, 18 hemi-mandibles and mandibles, and 13 sets of associated isolated teeth) and 155 of *Mesaceratherium paulhiacense* (73 isolated teeth; 82 from two maxillae, seven hemi-mandibles and mandibles, and nine sets of associated isolated teeth; see Supplementary 1). The number of teeth studied with each method depended on the associated constraints (e.g., only averaged-worn upper molars with cusps preserved on ectoloph profile for mesowear) and is detailed in Table 1. The sample for isotopic content is limited due to our focus on identifiable fragments (species and locus) as the method is destructive.

Mesowear

Mesowear is the categorization of gross dental wear into herbivore diet categories. Traditionally, it is based on scoring cusp shape and occlusal relief on upper molars (Fortelius and Solounias 2000). Here, we used the mesowear ruler developed by Mihlbachler et al. (2011) on horses (close relatives of rhinoceroses). This approach gives scores from 0 (high sharp) to 6 (low blunt; see Supplementary 2 Fig. 1). This method results in low scores for browsers (attrition – tooth-tooth-contact – dominated) and high scores for grazers (abrasion – tooth-diet-contact – dominated), while mixed-feeders have intermediate values. In contrast to most studies on mesowear, we consistently scored the paracone rather than the sharpest buccal cusp (metacone or paracone), as there are notable differences between these two cusps in rhinoceroses (Taylor et al. 2013; Hullot et al. 2021). Moreover, as mesowear scores can be affected both by age and hypsodonty (Fortelius and Solounias 2000), we only scored upper molars with an average wear (wear stages from 4 to 7

Table 1 Number of specimens studied by method and species of rhinocerotids from Ulm-Westtangente

	Protaceratherium minutum	*Mesaceratherium paulhiacense*
Mesowear	16	12
Microwear		
Grinding	21	11
Shearing	9	5
Enamel hypoplasia	317	149
Body mass	54	24
Stable isotopy ($\delta^{18}O$, $\delta^{13}C$)	3	5
Mortality curves	336	155

defined by Hillman-Smith et al. 1986). Eventually, we compared the hypsodonty index (height of m3 divided by its width; Janis 1988) of both species.

Dental Microwear Texture Analyses (DMTA)

Dental microwear texture analyses (DMTA) study dietary preferences at a short term scale (days to months; Hoffman et al. 2015). This technique examines the tooth surface and identifies wear patterns associated with different dietary categories. In this study, we followed a protocol adapted from Scott et al. (2005) using scale-sensitive fractal analyses. We selected well-preserved molars (upper and lower, left and right) and sampled wear facets from both phases of the mastication (grinding and shearing) on the same enamel band near the protocone, protoconid or hypoconid (see Supplemetary 2 Fig. 2). Facets were cleaned twice using a cotton swab soaked in acetone to remove dirt, grit and glue. Then we made two silicone molds (Coltene Whaledent PRESIDENT The Original Regular Body, ref. 60019939). The second one was used for the analyses described hereafter.

The facet was cut out of the mold, put flat under a Leica Map DCM8 profilometer (TRIDENT, PALEVOPRIM Poitiers), and scanned using white light confocal technology with a 100 × objective (Leica Microsystems; Numerical aperture: 0.90; working distance: 0.9 mm). Using LeicaMap (v.8.2; Leica Microsystems), we pre-treated the obtained scans (.plu files) as follows: inversion of the surface (as they come from negative replica), replacement of the missing points (i.e., non-measured, less than 1%) by the mean of the neighboring points, removal of aberrant peaks (automatic operators including a morphological filter see supplementary information in Merceron et al. 2016), leveling of the surface, removal of form (polynomial of degree 8), and selection of a 200 × 200 µm area (1551 × 1551 pixels) saved as a digital elevation model (.sur) to be used for DMTA. We conducted scale-sensitive fractal analyses on the selected surfaces (200 × 200 µm; see Supplementary 3) using MountainsMaps® (v.8.2). Our study will focus on the following texture variables, described in detail in Scott et al. (2006):

- anisotropy or exact proportion of length-scale anisotropy of relief (epLsar) is a measure of the orientation concentration of surface roughness; in MountainsMaps®, this parameter has been corrected (NewepLsar), as there was an error in the code of Toothfrax (software previously used for DMTA but not supported anymore; Calandra et al. 2022);
- complexity or area-scale fractal complexity (Asfc) assesses the roughness at a given scale;
- heterogeneity of the complexity (HAsfc) gives information of the variation of complexity at a given scale (here 3 × 3 and 9 × 9) within the studied 200 × 200 µm zone.

Body mass estimations

Body mass is linked to many physiological and ecological parameters (e.g., diet, metabolism, heat evacuation; Peters 1983; Owen-Smith 1988; Clauss et al. 2003). Many studies have established equations to estimate fossils' body mass based on various dental and limb bone proxies (see the review of Hopkins 2018). In this study, we opted to use multiple dental proxies, as we studied teeth for all other methods and as they are abundant and well preserved in the fossil record. Each dental proxy and its associated established equation are listed in Table 2 alongside with the corresponding references.

Hypoplasia

Hypoplasia is a permanent and sensitive defect of the enamel that has been correlated with stresses, in particular

Table 2 List of the dental proxies and the associated equations used to estimate body mass in this study. Measurements are in mm for all equations and give body mass in kg for Janis (1990) and in g otherwise.

Locus	Equation	Reference
m1		
	ln(mass) = 1.5133 × ln(m1 length x width) + 3.6515	Legendre (1989)
	log(mass) = 3.26 × log(m1 length/10) + 1.337	Janis (1990)
m2		
	log(mass) = 3.2 × log(m2 length/10) + 1.13	Janis (1990)
	log(mass) = 3.07 × log(m2 length) + 1.07	Damuth (1990)
M1		
	ln(mass) = 3.19 × ln(M1 length) + 2.1	Fortelius and Kappelman (1993)
M2		
	log(mass) = 3.18 × log(M2 length/10) + 1.091	Janis (1990)
	log(mass) = 3.03 × log(M2 length) + 1.06	Damuth (1990)
	ln(m) = 3.09 × ln(M2 length) + 2.14	Fortelius and Kappelman (1993)

environmental ones (Skinner and Pruetz 2012; Kierdorf et al. 2012; Upex and Dobney 2012). It is however non specific and can take several forms, the etiology of which is not well understood (Small and Murray 1978). In the literature, no standard protocol, nor threshold between normal and pathological enamel are available, so we followed a classical approach that consists in recording and categorizing the defects following the Fédération Dentaire Internationale (1982). This index recognizes three main types of defects: linear (line around the crown), pitted (restricted rounded defect), and aplasia (extended zone missing enamel; see Supplementary 2 Fig. 3). In parallel, we recorded several parameters (distance to enamel-dentin junction, width – if applicable – localization on the tooth, and severity). We studied all available identified cheek teeth, both deciduous and permanent, with the exception of very worn (wear stages 9 and 10 defined by Hillman-Smith et al. 1986) or damaged teeth (i.e., with limited to no enamel preserved) to limit the risk of false negatives. This resulted in the exclusion of 26 teeth (20 of *P. minutum* and six of *M. paulhiacense*) and left 466 teeth suitable to study hypoplasia.

Mortality curves and age structure

Mortality curves indicate the number of individuals from a sample dying at each age category. They are often used to study taphonomy (attritional causes) and to infer population structure in ancient communities (Fernandez and Legendre 2003; Bacon et al. 2018). Here, we used a protocol specifically designed for rhinocerotids detailed in Hullot and Antoine (2020). The age estimation is based on the correspondence between wear stages (1–10) and age classes (0-XVI) defined by Hillman-Smith et al. (1986) for each tooth locus. Mortality curves can then be built by following the steps thereafter:

- each tooth is considered individually and has a weight of 1;
- estimation of the wear stage (1 to 10) for each tooth;
- correlation to one or several age classes corresponding to the wear observed for the locus concerned;
- equal weight given to each age class (1 if one, ½ if two, and so on);
- for associated teeth, grouping of all teeth as a single individual and proposition of a class or combination of weighted classes for the group;
- construction of mortality curves from the weighted classes.

Based on the individual ages estimated following the steps above, we calculated the age structure of our sample. Ontogenetic stages were defined following the correlations from Hullot and Antoine (2020):

- juveniles (birth to weaning) include age classes from I to V, corresponding to 1.5 months to 3 years old in the extant white rhinoceros and ending with the eruption of the first permanent teeth (m1/M1);
- subadults (weaning to sexual maturity) correspond to age classes VI to VIII (i.e., 3 to 7 years), ending with the eruption of the last permanent teeth (m3/M3);
- adults (sexual maturity to death) correlates with age classes IX to XVI (i.e., 7 to 40 years), after the eruption of the last permanent teeth (m3/M3).

Minimum number of individuals

The minimum number of individuals (MNI) is the smallest number of individuals of the same species that can be identified from a fossil assemblage. It is determined by the number of the most abundant anatomical element from the same side (e.g., left femurs, right M3s). Here, estimations also took into account the incompatibility groups based on the pattern of dental eruption defined by Hullot and Antoine (2020). For instance, milk teeth are never associated in a functioning tooth row with the fourth premolar (group b) nor third molar (group a).

Isotopic analyses

Stables isotopes are often used in paleontology as they allow for dietary and environmental insights into terrestrial and aquatic ecosystems (Cerling et al. 1997; Clementz 2012). Here, we studied $\delta^{13}C$ – linked to the feeding behavior (C3-C4 plants) and to the habitat openness – and $\delta^{18}O$ – which depends on temperature and precipitation – of the carbonates from the dental enamel of both rhinocerotid species from Ulm-Westtangente. The $\delta^{18}O$ of rhinoceros enamel is especially interesting for climatic/environmental reconstructions as these animals were abundant and large sized, with a drinking behavior likely resulting in a $\delta^{18}O$ accurately recording the meteoritic precipitation of the area (Clauss et al. 2005; Levin et al. 2006; Martin et al. 2008; Zanazzi et al. 2022).

After mechanical cleaning of a small area of the tooth crown, we took samples on identified tooth fragments (taxon and locus) using a Dremmel© equipped with a diamond tip. We selected preferably third molars to avoid pre-weaning or weaning signal. Between 500 and 1000 µg of enamel powder were used for the analyses. Organic matter was removed following standard procedures (Cerling et al. 1997), and the samples were then acidified with phosphoric acid (103%), producing carbon monoxide to be analyzed for isotopic content using a Micromass Optima Isotope Ratio Mass Spectrometer (Géosciences Montpellier). Results detailed in Table 3 are expressed as ratio (‰) to the Vienna-Pee Dee Belemnite (V-PDB) standard as follows:

Table 3 Oxygen (O) and carbon (C) isotopic compositions of the enamel carbonates of Ulm-Westtangente rhinocerotids

Specimen	Weight (mg)	Tooth	Species	$\delta^{13}C_{CO3,\ enamel}$ (‰ V-PDB)	$\delta^{13}C_{CO3,\ enamel}$ Stdev	$\delta^{18}O_{CO3,\ enamel}$ (‰ V-PDB)	$\delta^{18}O_{CO3,\ enamel}$ Stdev
47950	628	M3	*P. minutum*	-7.47	0.01	-5.34	0.04
48079	520	M3	*P. minutum*	-8.25	0.02	-5.2	0.03
48184	580	M3	*P. minutum*	-8.51	0.04	-4.78	0.06
48072	628	m3	*M. paulhiacense*	-9.06	0.02	-5.15	0.04
48008	722	M1	*M. paulhiacense*	-10.77	0.02	-5.32	0.03
48183	502	P4	*M. paulhiacense*	-12.76	0.01	-6.04	0.02
47877	1054	M3	*M. paulhiacense*	-11.01	0.02	-5.29	0.02
47877	554	M1-2	*M. paulhiacense*	-9.47	0.01	-5.01	0.02

$$\delta = 1000 \times \left(\frac{R_{sample}}{R_{standard}} - 1\right)$$

where R_{sample} refers to the ratio of $\frac{^{13}C}{^{12}C}$ and $\frac{^{18}O}{^{16}O}$ of the sample and $R_{standard}$ to the Vienna-Pee Dee Belemnite standard. The within-run precision ($\pm 1\ \sigma$) of these analyses as determined by the replicate analyses of NBS 18 and AIEA-603 was less than ± 0.2 ‰ for $\delta^{13}C$ and ± 0.3 ‰ for $\delta^{18}O$ (n = 5–6 respectively).

The $\delta^{13}C_{diet}$ can be traced back from $\delta^{13}C_{CO3,\ enamel}$ taking into account the body mass and the digestive system (Tejada-Lara et al. 2018) as detailed below:

$$\varepsilon^*_{diet-bioapatite} = e^{2.42+0.032\times\ln(mass)}$$
$$\delta^{13}C_{diet} = \delta^{13}C_{CO3,enamel} - \varepsilon^*_{diet-bioapatite} - corr$$

where corr is the correction factor for the variation of $\delta^{13}C_{CO2}$ of the atmosphere, here equal to 1.9 ‰. Post 1930, the value of $\delta^{13}C_{CO2}$ in the atmosphere is -8 ‰ (Zachos et al. 2001). For Ulm-Westtangente, the reconstructed values based on benthic foraminifera at around 22 Mya are higher than today, with an estimate of -6.1 ‰ (Tipple et al. 2010).

The $\delta^{13}C_{diet}$ can in turn provide the mean annual precipitation (MAP) with the equation from Kohn (2010):

$$MAP = 10^{\left(\frac{-\delta^{13}C_{diet}+10.29+0.0124\times|latitude|-1.9\times10^{-4}\times altitude}{5.61}\right)} - 300$$

The $\delta^{18}O_{CO3(V\text{-}PDB)}$ was converted into $\delta^{18}O_{CO3(V\text{-}SMOW)}$ using the equation from Coplen et al. (1983) and where V-SMOW is the Vienna Standard Mean Ocean Water:

$$\delta^{18}O_{V-SMOW} = 1.03091 \times \delta^{18}O_{V-PDB} + 30.91$$

This was used to calculate the $\delta^{18}O_{precipitation}$ and the mean annual temperature (MAT) detailed as follows. No reliable equation to estimate the $\delta^{18}O_{precipitation}$ based on the $\delta^{18}O_{enamel}$ of rhinoceros is available in the literature. Tütken et al. (2006) tentatively established one, based on a dataset of extant rhinoceros (including zoo specimens), and using converted phosphates values obtained from the carbonates ones. The MATs obtained with this equation are consistently 2–4 °C higher (MH pers. obs.) than the ones estimated with equations specific to horses (Sánchez Chillón et al. 1994), bisons (Bernard et al. 2009), or elephants (Ayliffe et al. 1992). Hence, we decided to use the equation for modern elephants, as they might be the closest equivalent to rhinoceros for isotope fractionation due to similar metabolic requirements (e.g., large size, obligate drinkers). The $\delta^{18}O$ in the following equations are expressed in relation to the V-SMOW:

$\delta^{18}O_{PO4} = 0.94 \times \delta^{18}O_{precipitation} + 23.3$ equation from Ayliffe et al. (1992) for modern elephants.

$\delta^{18}O_{PO4} = 0.96 \times \delta^{18}O_{C03} - 8.05$ relation phosphates-carbonates from Lécuyer et al. (2010).

Hence: $\delta^{18}O_{precipitation} = 1.02 \times \delta^{18}O_{CO3} - 33.3$

Eventually, the MAT can be calculated using the obtained $\delta^{18}O_{precipitation}$ (Tütken et al. 2006):

$$MAT = \frac{\delta^{18}O_{precipitation} + 14.178}{0.442}$$

Statistics and figures

All statistics were conducted in R (R Core Team 2021: v. 4.1.2) equipped with the package tidyr (Wickham and Henry 2020), MASS (Ripley et al. 2013) and mvnormtest (Jarek 2012). Following the recent statement of the American Statistical Association (ASA) on p-values (Wasserstein and Lazar 2016), we favored giving exact values and we tried to be critical regarding the classical thresholds of "statistical significativity". Figures were done using R packages ggplot2 (Wickham 2016), cowplot (Wilke 2020), as well as Inkscape (v. 1.0.1).

Results

Structure of the rhinocerotid sample from Ulm-Westtangente

There are about twice as many teeth attributed to *Protaceratherium minutum* (337) than to *Mesaceratherium*

paulhiacense (155) at Ulm-Westtangente. The minimum number of individuals (MNI), based on dental remains, is 17 for *P. minutum* (number of left m1s) and 10 for *M. paulhiacense* (number of left p3s). When dental eruption incompatibility groups are considered, the MNIs are 24 (group b: fourth premolars and milk teeth) and 15 (group d: third milk molars and third premolars) respectively.

Before correction for the duration of the age classes, we observe a single peak centered around age class IX (7–9 yo in extant rhinoceros; Fig. 1A-B) for both species, although more spread out in *M. paulhiacense* (IX to XII; 7–20 yo). In the corrected mortality curves (i.e., number at each age class divided by the duration of the age class), similar tendencies were observed for both species (two-sided Kolmogorov–Smirnov test: D = 0.375, p-value = 0.2145), but with a smaller amplitude for the less abundant *M. paulhiacense*. The histograms of both species reveal four distinct peaks, around age classes I-II (1.5–4 months old), IV (1–1.5 yo), VI-VII (1.5–4 yo), and IX (7–9 yo; Fig. 1C-D).

The age structure of the rhinocerotid sample from Ulm-Westtangente with both species merged is composed by 10.8% of juveniles, 20.2% of subadults, and 69% of adults. The proportions were similar in both species (Chi2: X-squared = 0.32999, df = 2, p-value = 0.8479), with 10.5% of juveniles, 18.3% of subadults, and 71.2% of adults for *M. paulhiacense*, and 11% of juveniles, 21.2% of subadults, and 67.8% of adults for *P. minutum* (see details in Supplementary 1).

Enamel hypoplasia

At Ulm-Westtangente, a total of 79 teeth of the 466 examined for hypoplasia (16.95%) have at least one hypoplastic defect. However, there are differences in frequency between species and tooth loci (Fig. 2).

Both rhinocerotid species have similar overall hypoplasia prevalences (Kruskal–Wallis test: chi-squared = 0.044163, df = 1, p-value = 0.8336) with 16.7% (53/317) for *P. minutum* and 17.4% (26/149) for *M. paulhiacense*. Regarding tooth loci, when both species are merged, four are not affected (only milk molars), 14 have a prevalence of hypoplasia above 10% and seven above 20% (Table 4). In general, milk teeth are relatively spared (11.7 to 20% for D1, D2 and d3) or even not affected (0% of d1, d2, d4, and D4), with the notable exception of D3 for both species (species merged: 3/5, 40%), although the number of D3s is limited (Table 4).

The pattern of loci affected by hypoplasia was however different by species. For *P. minutum*, the most affected loci were the p3 (8/22; 36.4%), D3 (1/3; 33.3%), P3 (6/18; 33.3%), P2, and m3 (each 8/25; 32%), while d1, d2, D2, d3, d4, D4, M1, and M2 were never hypoplastic (Fig. 2). On the other hand, in *M. paulhiacense* the most affected loci were D3 (1/2; 50%), P4 (4/11; 36.4%), M2 (3/10; 30%), D1 (2/7;

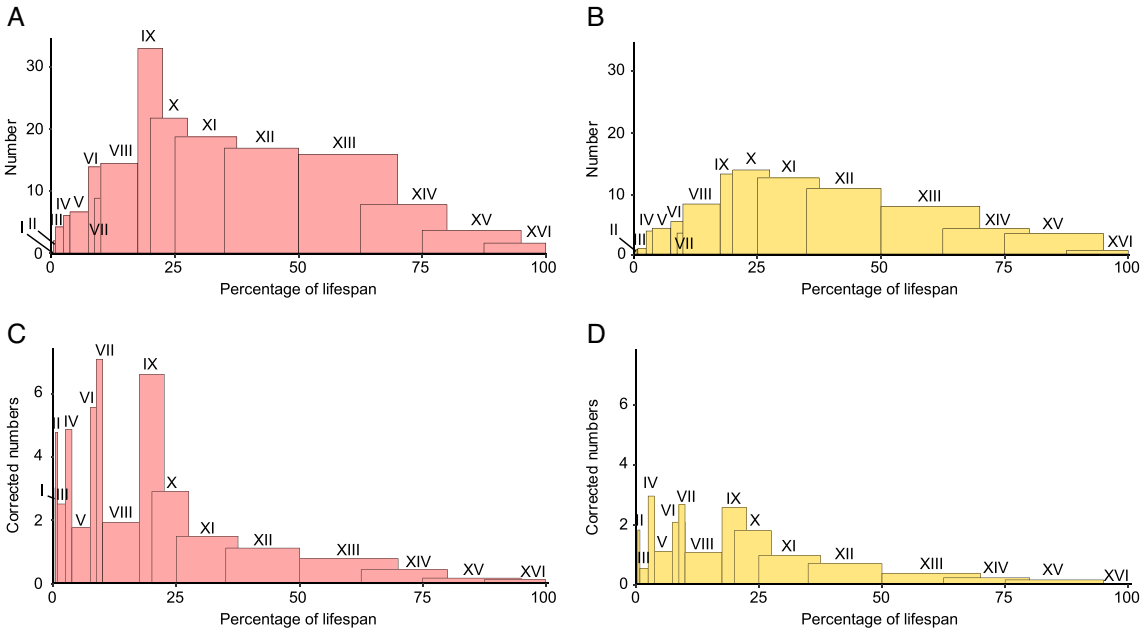

Fig. 1 Mortality curves of both rhinocerotid species from Ulm-Westtangente. Number of specimens per age class by species: A – *Protaceratherium minutum*, and B – *Mesaceratherium paulhiacense*. Correction for age class duration (number of specimens divided by the duration of the age class) by species: C – *Protaceratherium minutum*, and D – *Mesaceratherium paulhiacense*. Classes expressed as percentage of lifespan instead of age to limit actualism. Colour code: pink – *Protaceratherium minutum*, yellow – *Mesaceratherium paulhiacense*

Fig. 2 Number and frequency of hypoplasia by locus and species among the rhinocerotids from Ulm-Westtangente. Light colors for unaffected and dark for hypoplastic teeth. A – Number and frequency of hypoplastic teeth vs. unaffected ones for *Protaceratherium minutum*. B—Number and frequency of hypoplastic teeth vs. unaffected ones for *Mesaceratherium paulhiacense*

Table 4 Hypoplasia prevalence by locus (both species merged) at Ulm-Westtangente

Locus	d1	D1	d2	D2	d3	D3	d4	D4	p2	P2	p3	P3	p4	P4	m1	M1	m2	M2	m3	M3
Unaffected	17	16	13	5	15	3	11	6	25	27	26	21	32	18	34	19	29	20	25	25
Affected	0	4	0	1	2	2	0	0	1	10	11	7	7	6	4	2	5	3	10	4
Frequency	0	20	0	16.67	11.76	40	0	0	3.85	27.03	29.73	25	17.95	25	10.53	9.52	14.71	13.04	28.57	13.79

28.6%), D2 (1/4; 25%), d3 (2/8; 25%), and M1 (2/8; 25%), while d1, d2, d4, D4, p2, p4, and m1 were never hypoplastic (Fig. 2).

Body mass

Both species exhibit obvious differences in size, which is reflected in their body mass estimates, as detailed in Table 5. Mean estimates range from 438 to 685 kg for *P. minutum* and from 1389 to 2327 kg for *M. paulhiacense*, depending on the dental proxy and the equation applied.

Dietary preferences and habitat

Only a few unworn m3s were available to calculate the hypsodonty index (n = 5 for *P. minutum* and n = 3 for *M. paulhiacense*), but both species had relatively similar values (Kruskal–Wallis chi-squared = 1.0889, df = 1, p-value = 0.2967). However, according to the thresholds

Table 5 Body mass estimates (in kg) of the rhinocerotids from Ulm-Westtangente based on dental proxies. The number of teeth (n; only one per specimen if both were available) and the mean are shown for each proxy and species. Minimum and maximum estimates are indicated in bold for each species

	m1		m2		M1		M2	
	Legendre 1989	Janis 1990	Janis 1990	Damuth 1990	Fortelius and Kappelman 1993	Janis 1990	Damuth 1990	Fortelius and Kappelman 1993
Protaceratherium minutum								
n	19	19	16	16	10	9	9	9
mean	508.93	**685.34**	496.03	**438.11**	474.28	644.10	532.53	487.95
Mesaceratherium paulhiacense								
n	4	4	7	7	6	7	7	7
mean	**1389.20**	2043.93	2022.79	1687.06	1935.42	**2327.43**	1811.66	1700.52

established by Janis (1988), *P. minutum* classifies as brachyodont (mean hypsodonty index of 1.31), while *M. paulhiacense* is mesodont (mean hypsodonty index of 1.55). This could suggest a more abrasive diet for *M. paulhiacense*.

The mesowear scores were contrasted between the two species samples (Table 6; Kruskal–Wallis test: chi-squared = 5.2828, df = 1, p-value = 0.02154). *Protaceratherium minutum* (n = 16) had a mean ruler score of 1.75, with values ranging from 0 (n = 1) to 3 (n = 1). On the other hand, *Mesaceratherium paulhiacense* (n = 12) had a higher mean ruler score of 2.25 with values ranging from 1 (n = 2) to 4 (n = 5). This suggests a more abrasive diet for *M. paulhiacense*, consistent with the slightly higher hypsodonty index obtained above for this species (mesodont).

The dental microwear texture analyses (DMTA) revealed slightly contrasted results between grinding and shearing facets (MANOVA: p-value = 0.07842), but only for NewepLsar (ANOVA, p-value = 0.00621) and Asfc (ANOVA, p-value = 0.041). Regarding species, DMT signatures were relatively similar (Table 6; MANOVA: p-value = 0.65653), although some differences might be worth noting. The mean Asfc was lower for both facets of *M. paulhiacense* (Gr: 1.32; Sh: 0.77) than that of *P. minutum* (Gr: 1.72; Sh: 1.02), suggesting the processing of slightly softer food items by *M. paulhiacense*. On the grinding facet, *P. minutum* had higher mean values of HAsfc9 and HAsfc81 (0.37 and 0.68) than *M. paulhiacense* (0.24 and 0.40), but the opposite is observed for the shearing facet (HAsfc9: 0.29 for *P. minutum* vs 0.35 for *M. paulhiacense*; HAsfc81: 0.46 vs 0.58 respectively). This indicates a greater diversity of items consumed requiring grinding and a lower diversity of items consumed requiring shearing in *P. minutum*.

The isotopic content of the enamel carbonates for our rhinocerotid sample (n = 8) ranged between -12.76 and -7.47 ‰ for $\delta^{13}C_{CO3,\ enamel}$ and -6.04 and -4.78 for $\delta^{18}O_{CO3,\ enamel}$ (Table 3). Regarding $\delta^{18}O_{CO3,\ enamel}$, both rhinocerotids had similar means (Wilcoxon test; W = 6, p-value = 0.7857) with -5.1 ± 0.3 ‰ Vienna Pee Dee Belemnite (VPDB) for *P. minutum* and -5.4 ± 0.4 ‰ VPDB for *M. paulhiacense*, suggesting similar drinking water sources. The

Table 6 Dental wear signatures of the rhinocerotids from Ulm-Westtangente. When several teeth per specimen were available, only one tooth per specimen was studied, preferentially second molars. Gr: grinding facet, Sh: shearing facet, sd: standard deviation

	Protaceratherium minutum			*Mesaceratherium paulhiacense*		
	n	mean	sd	n	mean	sd
Mesowear	16	1.75	0.68	12	2.25	0.97
Microwear	Gr: 21 Sh: 9			Gr: 11 Sh: 5		
NewepLsar (10^{-2})		Gr: 1.67 Sh: 1.84	Gr: 0.17 Sh: 0.28		Gr: 1.70 Sh: 1.88	Gr: 0.12 Sh: 0.19
Asfc		Gr: 1.72 Sh: 1.02	Gr: 1.25 Sh: 0.67		Gr: 1.32 Sh: 0.77	Gr: 0.71 Sh: 0.22
HAsfc9		Gr: 0.37 Sh: 0.29	Gr: 0.44 Sh: 0.14		Gr: 0.24 Sh: 0.35	Gr: 0.07 Sh: 0.16
HAsfc81		Gr: 0.68 Sh: 0.46	Gr: 0.60 Sh: 0.13		Gr: 0.40 Sh: 0.58	Gr: 0.10 Sh: 0.25

mean $\delta^{18}O_{CO3,\ enamel}$ was however a little lower for *M. paulhiacense*, but this could be due to an outlier value (Fig. 3A; mean without outlier -5.2 ± 0.1 ‰ VPDB). The $\delta^{18}O_{precipitation}$ obtained from $\delta^{18}O_{SMOW}$ had a mean of -7.2 ± 0.2 ‰ (both species merged, outlier removed), which is significantly higher than today's values that are around -9.3 ‰ (today's value at Ulm, Germany calculated with the Online Isotopes in Precipitation Calculator: https://wateriso.utah.edu/waterisotopes/pages/data_access/oipc.html). The value obtained from the rhinocerotid specimens (both species merged, outlier removed) suggests a mean annual temperature (MAT) of 15.8 °C (see Supplementary 1 for all calculated values for each specimen).

Clear differences are observed between both species for $\delta^{13}C_{diet}$ (Wilcoxon test; W = 0, p-value = 0.03571), although they stay in the range of C3 feeding and habitats (Fig. 3). The values of *P. minutum* are higher (n = 3, mean = -23.7 ± 0.5 ‰) compared to those of *M. paulhiacense* (n = 5, mean = -26.8 ± 1.5 ‰). Without the outlier (*M. paulhiacense*, mean = -26.3 ± 1 ‰), the difference between the two species in the $\delta^{13}C_{diet}$ is less marked (Wilcoxon test; W = 0, p-value = 0.05714), but still suggests different dietary and/or habitat preferences. From the $\delta^{13}C_{diet}$ we calculated the mean annual precipitation (MAP). All specimens of *P. minutum* yielded negative MAPs, resulting from a pitfall in the equation (see discussion). The mean for *M. paulhiacense* (outlier excluded) gives a MAP of 317 mm/year (see Supplementary 1). The MAP calculated based on *M. paulhiacense* however shows great variations depending of the specimen (ranging from 84 to 556 mm/year). Such a result can be explained by the individual preferences, especially as *M. paulhiacense* is here reconstructed as a mixed-feeder and might have consumed a wide range of different food items.

Discussion

Body mass of the rhinocerotids from Ulm-Westtangente

In extant rhinoceros, one of the most accurate dental proxies appears to be the length of the M2 using the equation of Damuth (1990; MH pers. obs.). Applied to our dataset, the results are a mean of 532.5 kg for *P. minutum* and 1811.7 kg for *M. paulhiacense* (Table 5). Such a body mass for *P. minutum*, around 500 kg, is consistent with a previous estimation based on the astragalus (Becker 2003). In their study on Ulm-Westtangente, Costeur et al. (2012) used the occlusal surface of m1 as a proxy for body mass (Legendre 1989). They found higher means than our study using the same proxy for both species (590 vs. 509 kg and 1752 vs. 1389 kg respectively). Such discrepancies might result from an inter-observer bias, the inclusion of misidentified teeth (e.g., m2 instead of m1), a restricted data set in their study (sampling bias), or the inclusion of worn teeth in our study (rhinoceros m1 tend to shorten with wear; Antoine pers. comm., MH pers. obs.). In any case, the rhinocerotids are the biggest species found at Ulm-Westtangente (Costeur et al. 2012), with only *M. paulhiacense* exceeding 1000 kg, the threshold for megaherbivores following Owen-Smith (1988).

Age structure, stress vulnerability, and mortality of the rhinocerotids from Ulm-Westtangente

The age structure of both rhinocerotid samples exhibits approximately 10% of juveniles, 20% of subadults, and 70% of adults. This distribution closely aligns with the observed

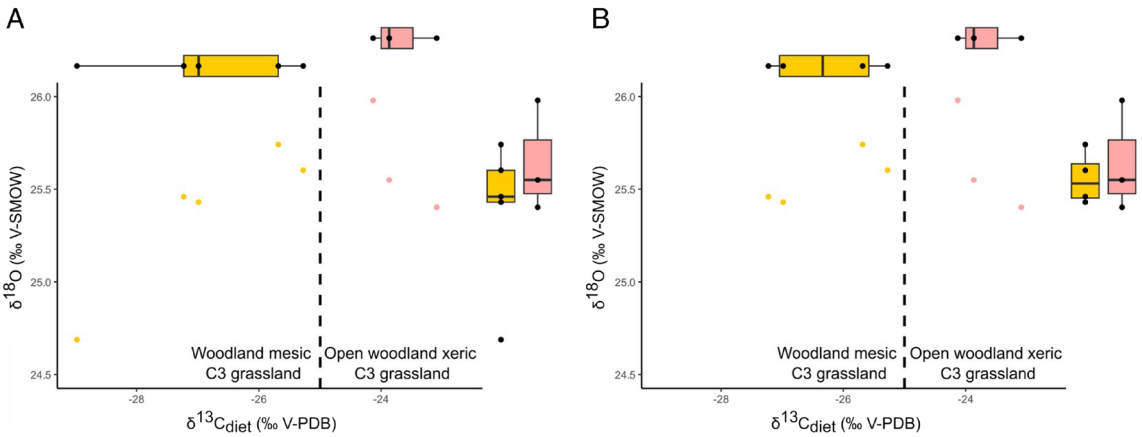

Fig. 3 Isotopic values of $\delta^{18}O_{CO3,\ SMOW}$ and $\delta^{13}C_{diet}$ for the two rhinocerotids from Ulm-Westtangente. A- Dotplot of $\delta^{18}O_{CO3,\ SMOW}$ against $\delta^{13}C_{diet}$ (corrected for body mass and for the variations of atmospheric $\delta^{13}C_{Co2}$) with associated boxplots. B- Same graph without the outlier of *Mesaceratherium paulhiacense*. One specimen of *M, paulhiacense* (48183) appeared as an outlier for $\delta.^{18}O_{CO3,\ SMOW}$ (outside whiskers range) and was removed as we suspected a weaning signal. Color code: pink- *Protaceratherium minutum* and yellow- *Mesaceratherium paulhiacense*. Threshold for modern plants and environments reported in Domingo et al. (2013)

age structure in modern *Diceros bicornis* populations (Supplementary 2 Fig. 4; Goddard 1970; Hitchins 1978). As Ulm-Westtangente provides a relatively time constrained framework (fossil layer only 35 cm thick; Heizmann et al. 1989), the studied sample could closely reflect living populations of both rhinocerotids with very minor preservation or taphonomical bias. The comparison with extant populations of rhinoceros must, however, be drawn with caution, as poaching and population management might have biased the observed age structure.

The mortality curves based on rhinocerotid teeth from Ulm-Westtangente (Fig. 1) suggested several vulnerability periods, similar in both species. The first peak is noted for classes I and II (0.31 to 0.83% of the lifespan, i.e. 1.5 to 4 months old in extant *Ceratotherium simum*; Hillman-Smith et al. 1986), and corresponds to the period shortly after birth. Birth is known to be a particularly stressful event in the life of an animal and newborns are very vulnerable (Upex and Dobney 2012). Stresses at birth have notably been correlated with the presence of a neonatal line in primate deciduous teeth and first molar (Gustafson and Gustafson 1967; Risnes 1998), as well as with hypoplasia on fourth milk molars in several ungulates (rhinoceros: Mead 1999; bison: Niven et al. 2004; sheep: Upex and Dobney 2012). In our data set fourth milk molars (d4/D4) are never affected in either species (Fig. 2). This finding is not necessarily contradicting, as the animal must survive the stress for the hypoplasia defect to be visible (Guatelli-Steinberg 2001). Other loci, that also develop around birth, displayed however a higher prevalence of hypoplasia, especially in *M. paulhiacense*. This is notably the case of the first upper molar (Tafforeau et al. 2007; Upex and Dobney 2012), which was amongst the most affected loci in *M. paulhiacense* (25% of M1; Fig. 2), or of other milk teeth loci suggesting early life stresses (or even in utero; Fig. 2).

The second peak is observed at age class IV (2.5 to 3.75% of the lifespan, i.e. 1 to 1.5 years old), which may be a sign of juvenile diseases. Hypoplasia in fossil rhinoceros has previously been linked to juvenile malnutrition or fever-causing diseases (Bratlund 1999), although no specific locus was mentioned. Based on the timing of tooth development in extant rhinoceros, hypoplasia due to juvenile diseases could impact all premolars and molars except the m3/M3 (chapter IV, page 131: Hullot 2021). All these loci are affected in our data set, with a variable prevalence depending on the species, but a direct correlation with juvenile diseases is not straight forward.

The third peak corresponds to age classes VI-VII (7.5 to 10% of the lifespan, i.e. 3 to 4 years old), which are correlated to the period shortly after weaning (Hullot and Antoine 2020), maybe indicating cow-calf separation. Weaning and cow-calf separation are known to be critical times for many extant mammals, including rhinoceroses. Indeed, at that time, adult size is not yet reached in rhinoceros (Owen-Smith 1988), leading to a higher predation risk (Brain et al. 1999). In parallel, rhinoceros calves might experience food stresses due to their new independence (Mead 1999). Interestingly, both events have been associated with hypoplastic defects in primates and pigs (Goodman and Rose 1990; Dobney and Ervynck 2000; Guatelli-Steinberg 2001; Skinner and Pruetz 2012). In fossil rhinoceroses, Mead (1999) supposed that hypoplasia on the fourth premolars might be associated with cow-calf separation. Here, fourth premolars are mildly to highly affected (15 to 36%) for both species (Fig. 2, Table 4), which could suggest that cow-calf separation was also a stressful event in these fossil species. Moreover, in modern rhinoceroses, second molars develop at a relatively similar timing than that of fourth premolars (Goddard 1970; Hitchins 1978; Hillman-Smith et al. 1986). Interestingly, P4 and M2 commonly bear at least one hypoplastic defect in *M. paulhiacense* (Fig. 2).

Eventually, a last peak in mortality is observed around classes IX-X (17.5 to 27.5% of the lifespan, i.e. 7 to 11 years old), correlating with sexual maturity (Hullot and Antoine 2020). In modern rhinoceroses, courtship and mating can be violent, including male fights for dominance, male rejection by the female, female chasing by males or mating wounds (Owen-Smith 1988; Dinerstein 2003), all of which could explain the increase of mortality observed for these age classes. However, potential stresses associated with this last peak were not recorded by enamel hypoplasia, as they occurred post-odontogenetically.

Paleoecology of the rhinocerotids from Ulm-Westtangente

Overall, results from carbon isotopic content, meso- and micro-wear suggest different dietary preferences for the two rhinocerotid species at Ulm-Westtangente. The carbon isotopic signal of both species falls in the range of C3 feeding (modern C3 ranging from -20 to -37 ‰; Kohn 2010), but points towards different habitats and/or dietary preferences (Fig. 3). Based on the thresholds between habitats established by Domingo et al. (2013), the $\delta^{13}C_{diet}$ values corrected for body mass and atmospheric $\delta^{13}C_{CO2}$ variations (see material and methods) indicate a more closed environment (woodland mesic C3 grassland) for *M. paulhiacense*, whereas *P. minutum* seems restricted to open woodland xeric C3 grassland (Fig. 3). This last finding is in line with what has been inferred based on morphology, as *Protaceratherium minutum* is described as a cursorial brachyodont species typical of forested, partially open environments (Becker 2003).

Regarding mesowear, *M. paulhiacense* has a higher mean score (2.25) than *P. minutum* (1.75), pointing towards a more abrasive diet (Table 6). Interestingly, *M. paulhiacense*

has a slightly higher hypsodonty index and is also bigger (Table 5), which is often associated to a supposedly higher tolerance to low quality, more fibrous and abrasive diet (Jarman-Bell principle; Clauss et al. 2013; Steuer et al. 2014). The mesowear values observed for *P. minutum* (mostly 1 or 2) are consistent with browsing but also overlap with mixed-feeding, whereas that for *M. paulhiacense* (2, 3 and 4) point towards mixed-feeding or grazing (Rivals et al. 2017). However, a C4-grazing is unlikely based on the isotopic signal (Fig. 3), the age and the situation of Ulm-Westtangente (C4 scarce or absent in the early Miocene of Germany; Strömberg 2011). Fewer differences were noted in the microwear pattern of both species (Table 6). The slight differences in DMT are rather consistent with the mesowear, and points towards browsing in *P. minutum* (high values of Asfc correlated with browsing; Scott et al. 2006), and mixed-feeding in *M. paulhiacense*.

Outlier in the stable isotope dataset: weaning signal?

One tooth of *M. paulhiacense* has significantly lower values for both $\delta^{13}C_{CO3,enamel}$ and $\delta^{18}O_{CO3,enamel}$ (Table 3) than the rest of the sampled teeth and, hence, was considered as an outlier. Interestingly, this is the only premolar of our data set (P4). Such different isotopic contents could be the result of a sampling in the pre-weaning part of the P4, as this tooth is known to partly develop before weaning in several extant rhinoceros species (Goddard 1970; Hitchins 1978; Hillman-Smith et al. 1986; Mead 1999). Indeed, milk has a higher $\delta^{18}O$ than drinking water due to the preferential loss of the light oxygen isotope (^{16}O) through expired and transcutaneous water vapor fluxes (Kohn et al. 1996), as well as a lower $\delta^{13}C$ than plants due to the presence of lipids, which are depleted in ^{13}C relatively to other macronutrients (DeNiro and Epstein 1977). The carbon depletion might however be relatively limited in the case of rhinoceros, as the milk of living individuals has a very low lipid content (Osthoff et al. 2021).

Associated fauna and paleoenvironment

Besides the two rhinocerotid species, the herbivore assemblage at Ulm-Westtangente includes two other perissodactyl species – a chalicothere (cf. *Metaschizotherium wetzleri*) and a tapir (*Paratapirus intermedius*) – five artiodactyl species, and 18 rodent and lagomorph species (Heizmann et al. 1989; Costeur et al. 2012). However, the body mass of all these species is significantly lower than that of the rhinocerotids, with only the chalicothere and the tapir ranging between 100 and 200 kg (Costeur et al. 2012), which limits potential competitive interactions. Unfortunately, no precise data is available on the paleoecology of these species at Ulm-Westtangente. However, schizotheriine chalicotheres are often reconstructed as open woodland dwellers (Heissig 1999), consuming leaves, fruits and maybe seeds and bark (Schulz et al. 2007; Semprebon et al. 2011) – which is relatively similar to our results for rhinocerotids – while tapirs prefer forested habitats and are typically folivores (DeSantis and MacFadden 2007).

Regarding environmental conditions, the MAP was around 317 mm/year suggesting rather dry conditions (Supplementary 1). Important individual variations were observed, which might point towards a certain seasonality or a varied diet. However, our sample is limited and restricted to a single taxon (Rhinocerotidae), and robust estimates of MAP require averaging over multiple species in a single locality (Kohn 2010). Moreover, *P. minutum* specimens yielded negative values of MAP. Some parameters might result in low to negative MAP, such as the consumption of C4 or the variation of C3 plant isotope compositions within a single locality (Kohn 2010).

Regarding temperature, the study of Costeur et al. (2012), took interest in the whole mammal fauna and proposed a cenogram. This study inferred an environment of a warm-temperate forest with grassland habitats at Ulm-Westtangente, but found quite a low MAT, around 7 °C. This MAT is similar to the one proposed for Montaigu-le-Blin (France; reference of MN2a) using the same approach. The authors note that this estimation is surprising, as the Aquitanian conditions are reconstructed as warm-temperate to subtropical (Zachos et al. 2001), and argue that this could be a remnant of the Mi-1 glaciation. Here, we found a MAT of about 16 °C based on the oxygen content of the carbonates of the enamel from the rhinocerotid sample. Although several complications exist in calculating absolute MAT from $\delta^{18}O_{precipitation}$ (see details in Zanazzi et al. 2022), this result is more consistent with the warm-temperate forest with grassland habitats inferred on species assemblage and cenogram (Costeur et al. 2012), the presence of ectothermic species (Costeur et al. 2012; Klembara et al. 2017), and with the global climate reconstructed at that time (Zachos et al. 2001; Westerhold et al. 2020).

The medium prevalence of hypoplasia in our sample (~ 17%) also suggests good environmental conditions, although some seasonality can be suspected. Indeed, m3 is amongst the most affected loci especially for *P. minutum* (Fig. 2, Table 4), and hypoplasia on third molars has been associated with environmental stresses such as seasonality (Franz-Odendaal et al. 2003; Skinner and Pruetz 2012; Upex and Dobney 2012). Periodic floods are supposed at Ulm-Westtangente and proposed as attritional causes (Heizmann et al. 1989). Such events might result in increased levels of stress through vegetation damage, habitat loss or displacement and decrease of water quality (e.g., Lake et al. 2006). Moreover, periodic floods have

already been linked to increased hypoplasia prevalence in rhinocerotids (Hullot et al. 2021). Besides external stressors, an effect of the diet and/or of phylogeny on stress susceptibility has been hypothesized in Miocene rhinocerotids from other sites (Hullot et al. 2023a, b). Here, both species are closely phylogenetically related (early diverging taxa of Aceratheriinae sensu lato for Antoine et al. 2010 or Rhinocerotinae *incertae sedis* for Tissier et al. 2020) and are similarly affected despite having different inferred diets (Table 6), suggesting that phylogeny might be the main driver.

Conclusion

In this article, we provided paleoecological insights for the two rhinocerotid species from the Early Miocene locality of Ulm-Westtangente (Germany). All dietary proxies (mesowear, microwear, $\delta^{13}C$) pointed towards different feeding preferences, with a more generalistic behavior (mixed-feeding) for the larger species *Mesaceratherium paulhiacense*. As the rhinocerotids were by far the biggest species at Ulm-Westtangente, competitive interactions with other herbivores might have been limited. However, the investigation of ecological preferences of the other species associated, especially the chalicothere cf. *Metaschizotherium wetzleri* and the tapir *Paratapirus intermedius*, would be interesting to clarify the use of resources. The prevalence of hypoplasia was similar in both species (~ 17%) – suggesting a potential greater influence of phylogeny than diet/ecology in stress susceptibility – but we noted specific differences in the loci affected. Vulnerability periods correlating with life events (birth, juvenile diseases, weaning and cow calf separation, and seasonality) were identified in the mortality curves, in accordance with some interpretations on hypoplasia origin. Regarding the paleoenvironment, the rhinocerotid sample studied gave a mean annual temperature (MAT) of 15.8 °C and mean annual precipitation of 317 mm/year, suggesting rather warm and dry conditions. This was in agreement with the previous inferences of a warm-temperate forest with grassland patches, but not with the cenogram at the locality, which suggested significantly lower MAT (7 °C). Thus, the inclusion of isotopic data from other taxa and/or the use of serial sampling might provide a more robust calculation and an insight into a potential seasonality.

Supplementary Information The online version contains supplementary material available at https://doi.org/10.1007/s00114-024-01893-w.

Acknowledgements We are grateful to Dr. Eli Amson the curator for fossil mammals at the SMNS for granting access to and providing inventory numbers for the specimens of Ulm-Westtangente. We are also indebted to Jérôme Surault (PALEVOPRIM Poitiers) for scanning several specimens of *P. minutum* used for the microwear analyses. Eventually we would like to thank the two anonymous reviewers for their constructive feedback on the previous version of this text.

Funding Open Access funding enabled and organized by Projekt DEAL. This study was funded by a post doctoral fellowship of the Alexander von Humboldt Foundation (Germany).

Declarations The authors have no relevant financial or non-financial interests to disclose.

Open Access This article is licensed under a Creative Commons Attribution 4.0 International License, which permits use, sharing, adaptation, distribution and reproduction in any medium or format, as long as you give appropriate credit to the original author(s) and the source, provide a link to the Creative Commons licence, and indicate if changes were made. The images or other third party material in this article are included in the article's Creative Commons licence, unless indicated otherwise in a credit line to the material. If material is not included in the article's Creative Commons licence and your intended use is not permitted by statutory regulation or exceeds the permitted use, you will need to obtain permission directly from the copyright holder. To view a copy of this licence, visit http://creativecommons.org/licenses/by/4.0/.

References

Antoine P-O, Becker D (2013) A brief review of Agenian rhinocerotids in Western Europe. Swiss J Geosci 106:135–146. https://doi.org/10.1007/s00015-013-0126-8

Antoine P-O, Downing KF, Crochet J-Y et al (2010) A revision of *Aceratherium blanfordi* Lydekker, 1884 (Mammalia: Rhinocerotidae) from the Early Miocene of Pakistan: Postcranials as a key. Zool J Linn Soc 160:139–194. https://doi.org/10.1111/j.1096-3642.2009.00597.x

Ayliffe LK, Lister AM, Chivas AR (1992) The preservation of glacial-interglacial climatic signatures in the oxygen isotopes of elephant skeletal phosphate. Palaeogeogr Palaeoclimatol Palaeoecol 99:179–191. https://doi.org/10.1016/0031-0182(92)90014-V

Bacon A-M, Antoine P-O, Huong NTM et al (2018) A rhinocerotid-dominated megafauna at the MIS6-5 transition: The late Middle Pleistocene Coc Muoi assemblage, Lang Son province, Vietnam. Quat Sci Rev 186:123–141. https://doi.org/10.1016/j.quascirev.2018.02.017

Becker D (2003) Paléoécologie et paléoclimats de la molasse du Jura (oligo-miocène). PhD Thesis, Université de Fribourg

Bernard A, Daux V, Lécuyer C et al (2009) Pleistocene seasonal temperature variations recorded in the $\delta^{18}O$ of *Bison priscus* teeth. EPSL 283:133–143. https://doi.org/10.1016/j.epsl.2009.04.005

Brain C, Forge O, Erb P (1999) Lion predation on black rhinoceros (*Diceros bicornis*) in Etosha National Park. Afr J Ecol 37:107–109. https://doi.org/10.1046/j.1365-2028.1999.00137.x

Bratlund B (1999) Taubach revisited. Jahrbuch RGZM 46:61–174. https://doi.org/10.11588/jrgzm.1999.1.25776

de Bruijn H, Daams R, Daxner-Höck G et al (1992) Report of the RCMNS working group on fossil mammals, Reisensburg 1990. Newsl Stratigr 26:65–118. https://doi.org/10.1127/nos/26/1992/65

Calandra I, Bob K, Merceron G et al (2022) Surface texture analysis in Toothfrax and MountainsMap® SSFA module: Different software packages, different results? PCJ 2: e77. https://doi.org/10.24072/pcjournal.204

Cerling TE, Harris JM, Ambrose SH et al (1997) Dietary and environmental reconstruction with stable isotope analyses of herbivore tooth enamel from the Miocene locality of Fort Ternan, Kenya. J Hum Evol 33:635–650. https://doi.org/10.1006/jhev.1997.0151

Clauss M, Frey R, Kiefer B et al (2003) The maximum attainable body size of herbivorous mammals: Morphophysiological constraints on foregut, and adaptations of hindgut fermenters. Oecologia 136:14–27. https://doi.org/10.1007/s00442-003-1254-z

Clauss M, Polster C, Kienzle E et al (2005) Energy and mineral nutrition and water intake in the captive Indian rhinoceros (*Rhinoceros unicornis*). Zoo Biol 24:1–14. https://doi.org/10.1002/zoo.20032

Clauss M, Steuer P, Müller DWH et al (2013) Herbivory and body size: Allometries of diet quality and gastrointestinal physiology, and implications for herbivore ecology and dinosaur gigantism. PLoS One 8:e68714. https://doi.org/10.1371/journal.pone.0068714

Clementz MT (2012) New insight from old bones: Stable isotope analysis of fossil mammals. J Mammal 93:368–380. https://doi.org/10.1644/11-MAMM-S-179.1

Coplen TB, Kendall C, Hopple J (1983) Comparison of stable isotope reference samples. Nature 302:236–238. https://doi.org/10.1038/302236a0

Costeur L, Maridet O, Peigné S, Heizmann EP (2012) Palaeoecology and palaeoenvironment of the aquitanian locality Ulm-westtangente (MN2, lower freshwater molasse, Germany). Swiss J Palaeontol 131:183–199. https://doi.org/10.1007/s13358-011-0034-3

Damuth J (1990) Problems in estimating body masses of archaic ungulates using dental measurements. In: Damuth J, MacFadden BJ (eds) Body size in mammalian paleobiology: Estimation and biological implications. Cambridge University Press, Cambridge. pp 229–254

DeNiro MJ, Epstein S (1977) Mechanism of carbon isotope fractionation associated with lipid synthesis. Science 197:261–263. https://doi.org/10.1126/science.327543

DeSantis LR, MacFadden B (2007) Identifying forested environments in deep time using fossil tapirs: Evidence from evolutionary morphology and stable isotopes. CFS 258:147–157

Dinerstein E (2003) The return of the unicorns: The natural history and conservation of the greater one-horned rhinoceros. Columbia University Press, New-York

Dobney K, Ervynck A (2000) Interpreting developmental stress in archaeological pigs: The chronology of linear enamel hypoplasia. J Archaeol Sci 27:597–607. https://doi.org/10.1006/jasc.1999.0477

Domingo L, Koch PL, Fernández MH et al (2013) Late neogene and Early Quaternary paleoenvironmental and paleoclimatic conditions in southwestern Europe: Isotopic analyses on mammalian taxa. PLoS One 8:e63739. https://doi.org/10.1371/journal.pone.0063739

Fédération Dentaire Internationale (1982) An epidemiological index of development defects of dental enamel (DDE index). Int Dent J 42:411–426

Fernandez P, Legendre S (2003) Mortality curves for horses from the middle Palaeolithic site of bau de l'aubesier (Vaucluse, France): Methodological, palaeo-ethnological, and palaeo-ecological approaches. J Archaeol Sci 30:1577–1598. https://doi.org/10.1016/S0305-4403(03)00054-2

Fortelius M, Kappelman J (1993) The largest land mammal ever imagined. Zool J Linn Soc 108:85–101. https://doi.org/10.1006/zjls.1993.1018

Fortelius M, Solounias N (2000) Functional characterization of ungulate molars using the abrasion-attrition wear gradient: A new method for reconstructing paleodiets. Am Mus Novit 2000:1–36

Franz-Odendaal TA, Lee-Thorp JA, Chinsamy A (2003) Insights from stable light isotopes on enamel defects and weaning in pliocene herbivores. J Biosci 28:765–773. https://doi.org/10.1007/BF02708437

Goddard J (1970) Age criteria and vital statistics of a black rhinoceros population. Afr J Ecol 8:105–121. https://doi.org/10.1111/j.1365-2028.1970.tb00834.x

Goodman AH, Rose JC (1990) Assessment of systemic physiological perturbations from dental enamel hypoplasias and associated histological structures. Am J Phys Anthropol 33:59–110. https://doi.org/10.1002/ajpa.1330330506

Guatelli-Steinberg D (2001) What can developmental defects of enamel reveal about physiological stress in nonhuman primates? Evol Anthropol 10:138–151. https://doi.org/10.1002/evan.1027

Gustafson G, Gustafson AG (1967) Microanatomy and histochemistry of enamel. Structural and chemical organization of teeth. Academic Press, New York, pp 75–134

Heissig K (1999) Family chalicotheriidae. In: Rössner GE, Heissig K (eds) The miocene land mammals of Europe. Verlag Dr. Friedrich Pfeil, München, Germany, pp 189–192

Heizmann EP, Bloos G, Bloos G, Böttcher R (1989) Ulm-westtangente und Ulm-uniklinik: zwei neue wirbeltier-faunen aus der unteren süßwasser-molasse (untermiozän) von Ulm (baden-württemberg). Stutt Beitr Naturkd, B 153:1–14

Heizmann EP, Morlo M (1994) *Amphictis schlosseri* n. sp.-eine neue carnivoren-art (mammalia) aus dem unter-miozän von südwestdeutschland. Stutt Beitr Naturkd, B 216:1–25

Hellmund M (1991) Schweineartige (Suina, artiodactyla, mammalia) aus oligo-miozänen fundstellen deutschlands, der schweiz und frankreichs: I. *Hyotherium meissneri* (suidae) aus dem untermiozän von Ulm-westtangente (baden-württemberg). Stuttg Beitr Naturkunde Ser B 176:1–69

Hillman-Smith AKK, Owen-Smith NR, Anderson JL et al (1986) Age estimation of the white rhinoceros (*Ceratotherium simum*). J Zool 210:355–377

Hitchins PM (1978) Age determination of the black rhinoceros (*Diceros bicornis* Linn.) in Zululand. S Afr Wildl Res 8:71–80

Hoffman JM, Fraser D, Clementz MT (2015) Controlled feeding trials with ungulates: A new application of in vivo dental molding to assess the abrasive factors of microwear. J Exp Biol 218:1538–1547. https://doi.org/10.1242/jeb.118406

Hopkins SSB (2018) Estimation of body size in fossil mammals. In: Croft DA, Su DF, Simpson SW (eds) Methods in paleoecology: Reconstructing cenozoic terrestrial environments and ecological communities. Springer International Publishing, Cham, pp 7–22

Hullot M (2021) Analyses texturales des micro-usures et des hypoplasies de l'émail dentaire chez les Rhinocerotidae actuels et fossiles (Mammalia, Perissodactyla) : Inférences paléobiologiques et paléoécologiques. PhD thesis, Université Montpellier

Hullot M, Antoine P-O (2020) Mortality curves and population structures of late early Miocene rhinocerotidae (mammalia, perissodactyla) remains from the béon 1 locality of Montréal-Du-Gers, France. Palaeogeogr Palaeoclimatol Palaeoecol 558:109938. https://doi.org/10.1016/j.palaeo.2020.109938

Hullot M, Antoine P-O, Spassov N et al (2023a) Late Miocene rhinocerotids from the Balkan-Iranian province: Ecological insights from dental microwear textures and enamel hypoplasia. Hist Biol 35:1417–1434. https://doi.org/10.1080/08912963.2022.2095910

Hullot M, Laurent Y, Merceron G, Antoine P-O (2021) Paleoecology of the Rhinocerotidae (Mammalia, Perissodactyla) from Béon 1, Montréal-du-Gers (late early Miocene, SW France): Insights from dental microwear texture analysis, mesowear, and enamel hypoplasia. Palaeontol Electron 24:1–26. https://doi.org/10.26879/1163

Hullot M, Merceron G, Antoine P-O (2023b) Spatio-temporal diversity of dietary preferences and stress sensibilities of early and middle

Miocene Rhinocerotidae from Eurasia: impact of climate changes. PCJ 3:e5. https://doi.org/10.24072/pcjournal.222
Janis CM (1988) An estimation of tooth volume and hypsodonty indices in ungulate mammals, and the correlation of these factors with dietary preferences. Mém Mus Natl Hist Nat, Sér C 53:367–387
Janis CM (1990) Correlation of cranial and dental variables with body size in ungulates and macropodoids. In: Damuth J, MacFadden BJ (eds) Body size in mammalian paleobiology: Estimation and biological implications. Cambridge University Press, Cambridge, pp 255–300
Jarek S (2012) mvnormtest: Normality test for multivariate variables. R package version 0.1–9. https://cran.r-project.org/web/packages/mvnormtest/mvnormtest.pdf
Kierdorf H, Witzel C, Upex B et al (2012) Enamel hypoplasia in molars of sheep and goats, and its relationship to the pattern of tooth crown growth. J Anat 220:484–495. https://doi.org/10.1111/j.1469-7580.2012.01482.x
Klembara J, Hain M, Čerňanskỳ A (2017) The first record of anguine lizards (Anguimorpha, anguidae) from the early Miocene locality Ulm-Westtangente in Germany. Hist Biol 31:1016–1027. https://doi.org/10.1080/08912963.2017.1416469
Kohn MJ (2010) Carbon isotope compositions of terrestrial C3 plants as indicators of (paleo)ecology and (paleo)climate. PNAS 107:19691–19695. https://doi.org/10.1073/pnas.1004933107
Kohn MJ, Schoeninger MJ, Valley JW (1996) Herbivore tooth oxygen isotope compositions: Effects of diet and physiology. Geochim Cosmochim Acta 60:3889–3896. https://doi.org/10.1016/0016-7037(96)00248-7
Lake S, Bond N, Reich P (2006) Floods down Rivers: From damaging to replenishing forces. Adv Ecol Res 39:41–62. https://doi.org/10.1016/S0065-2504(06)39003-4
Lécuyer C, Balter V, Martineau F et al (2010) Oxygen isotope fractionation between apatite-bound carbonate and water determined from controlled experiments with synthetic apatites precipitated at 10–37°C. Geochim Cosmochim Acta 74:2072–2081. https://doi.org/10.1016/j.gca.2009.12.024
Legendre S (1989) Les communautés de mammifères du Paléogène (Eocène supérieur et Oligocène) d'Europe occidentale : Structures, milieux et évolution. Münchner Geowissenschaftliche Abhandlungen, München, Germany
Levin NE, Cerling TE, Passey BH et al (2006) A stable isotope aridity index for terrestrial environments. PNAS 103:11201–11205. https://doi.org/10.1073/pnas.0604719103
Martin C, Bentaleb I, Kaandorp R et al (2008) Intra-tooth study of modern rhinoceros enamel $\delta^{18}O$: Is the difference between phosphate and carbonate $\delta^{18}O$ a sound diagenetic test? Palaeogeogr Palaeoclimatol Palaeoecol 266:183–189. https://doi.org/10.1016/j.palaeo.2008.03.039
Mead AJ (1999) Enamel hypoplasia in Miocene rhinoceroses (*Teleoceras*) from Nebraska: Evidence of severe physiological stress. J Vertebr Paleontol 19:391–397. https://doi.org/10.1080/02724634.1999.10011150
Merceron G, Ramdarshan A, Blondel C et al (2016) Untangling the environmental from the dietary: Dust does not matter. Proc R Soc B 283:20161032. https://doi.org/10.1098/rspb.2016.1032
Mihlbachler MC, Rivals F, Solounias N, Semprebon GM (2011) Dietary change and evolution of horses in North America. Science 331:1178–1181. https://doi.org/10.1126/science.1196166
Niven LB, Egeland CP, Todd LC (2004) An inter-site comparison of enamel hypoplasia in bison: Implications for paleoecology and modeling Late Plains Archaic subsistence. J Archaeol Sci 31:1783–1794. https://doi.org/10.1016/j.jas.2004.06.001
Osthoff G, Beukes B, Steyn AC et al (2021) Milk composition of white rhinoceros over lactation and comparison with other Perissodactyla. Zoo Biol 40:417–428. https://doi.org/10.1002/zoo.21618
Owen-Smith NR (1988) Megaherbivores: The influence of very large body size on ecology. Cambridge University Press, Cambridge
Peigné S, Heizmann PJ (2003) The amphicyonidae (Mammalia: Carnivora) from Ulm-Westtangente MN2, Early Miocene), Baden-Württemberg, Germany: Systematics and ecomorphology. Stutt Beitr Naturkd, B 343:1
Peters RH (1983) The ecological implications of body size. Cambridge University Press, Cambridge
Raffi I, Wade BS, Pälike H et al (2020) The Neogene period. In: Gradstein FM, Ogg JG, Schmitz M, Ogg GM (eds) Geologic time scale 2020. Elsevier, Amsterdam, pp 1141–1215
Ripley B, Venables B, Bates DM et al (2013) Package 'mass.' Cran R 538:113–120
Risnes S (1998) Growth tracks in dental enamel. J Hum Evol 35:331–350. https://doi.org/10.1006/jhev.1998.0229
Rivals F, Uzunidis A, Sanz M, Daura J (2017) Faunal dietary response to the Heinrich event 4 in southwestern Europe. Palaeogeogr Palaeoclimatol Palaeoecol 473:123–130. https://doi.org/10.1016/j.palaeo.2017.02.033
Sánchez Chillón B, Alberdi MT, Leone G et al (1994) Oxygen isotopic composition of fossil equid tooth and bone phosphate: An archive of difficult interpretation. Palaeogeogr Palaeoclimatol Palaeoecol 107:317–328. https://doi.org/10.1016/0031-0182(94)90103-1
Schulz E, Fahlke JM, Merceron G, Kaiser TM (2007) Feeding ecology of the chalicotheriidae (Mammalia, perissodactyla, ancylopoda). Results from dental micro-and mesowear analyses. Verh Naturwiss Ver Hamburg 43:5–31
Scott RS, Ungar PS, Bergstrom TS et al (2005) Dental microwear texture analysis shows within-species diet variability in fossil hominins. Nature 436:693–695. https://doi.org/10.1038/nature03822
Scott RS, Ungar PS, Bergstrom TS et al (2006) Dental microwear texture analysis: Technical considerations. J Hum Evol 51:339–349. https://doi.org/10.1016/j.jhevol.2006.04.006
Semprebon GM, Sise PJ, Coombs MC (2011) Potential bark and fruit browsing as revealed by stereomicrowear analysis of the peculiar clawed herbivores known as chalicotheres (Perissodactyla, chalicotherioidea). J Mammal Evol 18:33–55. https://doi.org/10.1007/s10914-010-9149-3
Skinner MF, Pruetz JD (2012) Reconstruction of periodicity of repetitive linear enamel hypoplasia from perikymata counts on imbricational enamel among dry-adapted chimpanzees (*Pan troglodytes verus*) from Fongoli, Senegal. Am J Phys Anthropol 149:468–482. https://doi.org/10.1002/ajpa.22145
Small BW, Murray JJ (1978) Enamel opacities: Prevalence, classifications and aetiological considerations. J Dent 6:33–42. https://doi.org/10.1016/0300-5712(78)90004-0
Steininger FF (1999) Chronostratigraphy, geochronology and biochronology of the Miocene" European Land Mammal Mega-Zones"(ELMMZ) and the Miocene" Mammal-Zones (MN-Zones)". In: Rössner GE, Heissig K (eds) The miocene: Land mammals of Europe. Verlag Dr. Friedrich Pfeil, München, Germany, pp 9–24
Steuer P, Südekum K-H, Tütken T et al (2014) Does body mass convey a digestive advantage for large herbivores? Funct Ecol 28:1127–1134. https://doi.org/10.1111/1365-2435.12275
Strömberg CA (2011) Evolution of grasses and grassland ecosystems. Annu Rev Earth Planet Sci 39:517–544. https://doi.org/10.1146/annurev-earth-040809-152402
Tafforeau P, Bentaleb I, Jaeger J-J, Martin C (2007) Nature of laminations and mineralization in rhinoceros enamel using histology and X-ray synchrotron microtomography: Potential implications for palaeoenvironmental isotopic studies. Palaeogeogr Palaeoclimatol Palaeoecol 246:206–227. https://doi.org/10.1016/j.palaeo.2006.10.001

Taylor LA, Kaiser TM, Schwitzer C et al (2013) Detecting intercusp and inter-tooth Wear patterns in rhinocerotids. PLoS One 8:e80921. https://doi.org/10.1371/journal.pone.0080921

Tejada-Lara JV, MacFadden BJ, Bermudez L et al (2018) Body mass predicts isotope enrichment in herbivorous mammals. Proc R Soc B 285:20181020. https://doi.org/10.1098/rspb.2018.1020

Tipple BJ, Meyers SR, Pagani M (2010) Carbon isotope ratio of Cenozoic CO2: A comparative evaluation of available geochemical proxies. Paleoceanogr Paleoclimatol 25. https://doi.org/10.1029/2009PA001851

Tissier J, Antoine P-O, Becker D (2020) New material of *Epiaceratherium* and a new species of *Mesaceratherium* clear up the phylogeny of early rhinocerotidae (perissodactyla). R Soc Open Sci 7:200633. https://doi.org/10.1098/rsos.200633

Tütken T, Vennemann TW, Janz H, Heizmann EPJ (2006) Palaeoenvironment and palaeoclimate of the Middle Miocene lake in the Steinheim basin, SW Germany: A reconstruction from C, O, and Sr isotopes of fossil remains. Palaeogeogr Palaeoclimatol Palaeoecol 241:457–491. https://doi.org/10.1016/j.palaeo.2006.04.007

Upex B, Dobney K (2012) Dental enamel hypoplasia as indicators of seasonal environmental and physiological impacts in modern sheep populations: A model for interpreting the zooarchaeological record. J Zool 287:259–268. https://doi.org/10.1111/j.1469-7998.2012.00912.x

Wasserstein RL, Lazar NA (2016) The ASA statement on p-values: Context, process, and purpose. Am Stat 70:129–133. https://doi.org/10.1080/00031305.2016.1154108

Werner J (1994) Beiträge zur biostratigraphie der unteren süßwassermolasse süddeutschlands: Rodentia und lagomorpha (mammalia) aus den fundstellen der Ulmer gegend. Stutt Beitr Naturkd, B 200:1–263

Westerhold T, Marwan N, Drury AJ et al (2020) An astronomically dated record of earth's climate and its predictability over the last 66 million years. Science 369:1383–1387. https://doi.org/10.1126/science.aba6853

Wickham H (2016) ggplot2: Elegant graphics for data analysis. Springer-Verlag, New York

Wickham H, Henry L (2020) Tidyr: Tidy messy data. R package version 1:397. https://cran.r-project.org/web/packages/tidyr/index.html

Wilke CO (2020) cowplot: Streamlined plot theme and plot annotations for "ggplot2". R package version 110. https://CRAN.R-project.org/package=cowplot

Zachos JC, Shackleton NJ, Revenaugh JS et al (2001) Climate response to orbital forcing across the oligocene-miocene boundary. Science 292:274–278. https://doi.org/10.1126/science.1058288

Zanazzi A, Fletcher A, Peretto C, Thun Hohenstein U (2022) Middle Pleistocene paleoclimate and paleoenvironment of Central Italy and their relationship with hominin migrations and evolution. Quat Int 619:12–29. https://doi.org/10.1016/j.quaint.2022.01.011

Ziegler R (1989) Heterosoricidae und Soricidae (Insectivora, mammalia) aus dem Oberoligozan und untermiozan suddeutschlands. Stutt Beitr Naturkd, B 154:1–73

Ziegler R (1990a) Didelphidae, erinaceidae, metacodontidae und dimylidae (mammalia) aus dem oberoligozän und untermiozän süddeutschlands. Stutt Beitr Naturkd, B 158:1–99

Ziegler R (1990b) Talpidae (Insectivora, mammalia) aus dem oberoligozän und untermiozän süddeutschlands. Stutt Beitr Naturkd, B 167:1–59

Publisher's Note Springer Nature remains neutral with regard to jurisdictional claims in published maps and institutional affiliations.